diversity

MDPI

Article

Low Temperature Scanning Electron Microscopy (LTSEM) Findings on the Ultrastructure of *Trebouxia lynnae* (*Trebouxiophyceae*, Lichenized Microalgae)

César Daniel Bordenave [1,*], Francisco García-Breijo [2], Ayelén Gazquez [1], Lucía Muggia [3], Pedro Carrasco [4] and Eva Barreno [1]

[1] Instituto Cavanilles de Biodiversidad y Biología Evolutiva (ICBiBE), Botánica, Universitat de València, C/Dr. Moliner, 50, 46100 Burjassot, Spain
[2] Departamento de Ecosistemas Agroforestales ETSIAMN, Universitat Politècnica de València, Camino de Vera s/n, 46022 València, Spain
[3] Department of Life Sciences, University of Trieste, via L. Giorgieri 10, 34127 Trieste, Italy
[4] Instituto de Biotecnología y Biomedicina (BIOTECMED), Universitat de València, 46100 Burjassot, Spain
* Correspondence: cesar.bordenave@uv.es

Abstract: The lichenized green microalga *Trebouxia lynnae* Barreno has been recently described and is considered a model organism for studying lichen chlorobionts. Its cellular ultrastructure has already been studied in detail by light, electron, and confocal microscopy, and its nuclear, chloroplast and mitochondrial genomes have been sequenced and annotated. Here, we investigated in detail the ultrastructure of in vitro grown cultures of *T. lynnae* observed by Low Temperature Scanning Electron Microscopy (LTSEM) applying a protocol with minimum intervention over the biological samples. This methodology allowed for the discovery of ultrastructural features previously unseen in *Trebouxiophyceae* microalgae. In addition, original Transmission Electron Microscopy (TEM) images of *T. lynnae* were reinterpreted based on the new information provided by LTSEM. The nucleolar vacuole, dictyosomes, and endoplasmic reticulum were investigated and reported for the first time in *T. lynnae* and most likely in other *Trebouxia* lineages.

Keywords: axenic cultures; low temperature scanning electron microscopy; phycobiont; transmission electron microscopy

Citation: Bordenave, C.D.; García-Breijo, F.; Gazquez, A.; Muggia, L.; Carrasco, P.; Barreno, E. Low Temperature Scanning Electron Microscopy (LTSEM) Findings on the Ultrastructure of *Trebouxia lynnae* (*Trebouxiophyceae*, Lichenized Microalgae). *Diversity* **2023**, *15*, 170. https://doi.org/10.3390/d15020170

Academic Editor: Michael Wink

Received: 2 December 2022
Revised: 16 January 2023
Accepted: 21 January 2023
Published: 26 January 2023

1. Introduction

Lichens are self-sustaining microecosystems formed by the interaction of a major ascomycetous or basidiomycetous fungus (the mycobiont), photosynthetic microorganisms (the photobionts) comprising one or more populations of microalgae (phycobionts) and/or cyanobacteria (cyanobionts), and other microorganisms such as bacteria and other microfungi (filamentous and yeasts) [1]. In the lichen, the mycobiont builds a framework of hyphae enwrapping the photobionts cells, housing all the microorganisms that participate in the symbiosis. The genus *Trebouxia* Puymaly (*Trebouxiaceae*) comprises coccoid, colony-forming, aero-terrestrial green microalgae [2–5]. *Trebouxia* species are among the most widespread phycobionts, associating with a variety of ascomycetous mycobionts [6,7]. Among them, *Trebouxia lynnae* Barreno has emerged as the *Trebouxia* research model because its ultrastructure has been largely analysed and its cells have been described in detail by different approaches [8,9]. Furthermore, its nuclear, chloroplast, and mitochondrial genomes have been sequenced and annotated, and more physiology information is gathered every year [8–15].

The phycobiont-mycobiont association and their reciprocal selectivity are complex subjects. There are plenty of examples of phycobionts switching in relation to environmental and geographic variables. In particular, a diversity of *Trebouxia* phycobionts within different

lichen species has been reported across niche gradients [16–21]. In addition, the intrathalline coexistence of various *Trebouxia* species-level lineages has been frequently reported, and it has been suggested that the thallus morphology and growth stage affect the diversity of the associated phycobionts [12,17,22–28]. Inter- and intrathalline phycobiont diversity has been mainly assessed by molecular techniques [19,21,22,24–29]. The lack of additional evidence for phycobiont diversity gives rise to some questions: are we underestimating the phycobiont diversity by skipping photobionts with abundances below the detection threshold? Are there phycobionts undetectable by the molecular approaches due to the primers efficiency? Are less abundant phycobionts real symbionts, or rather residual cells of a former phycobiont? Are estimated phycobiont abundances reliable? Supplementing molecular analysis with taxonomic identification of microalgae inside the thalli by means of microscopy is highly desirable. To this end, it is essential to analyse the morphology and ultrastructure of putative species-level lineages and identify taxonomic relevant traits. In order to reliably identify phycobionts, it is important to correlate the in vitro traits with those exhibited in the symbiotic state within the lichen thallus [30].

Recently, the diversity and the evolutionary relationships of *Trebouxia* species-level lineages were reappraised by Muggia et al. [7], who assembled DNA sequence data from over 1600 specimens and inferred a phylogeny from multi-locus sequence data. The multi-locus phylogenetic reconstructions confirmed four major clades within *Trebouxia*. In Bordenave et al. [9], 20 axenically grown species-level lineages of *Trebouxia* belonging to the four major clades were characterized in their morphology and ultrastructure by Confocal Laser Scanning Microscopy (CLSM) and Transmission Electron Microscopy (TEM). Pyrenoid ultrastructure and chloroplast morphology were presented as reliable taxonomic recognition tools in the genus *Trebouxia*. However, it is possible to further distinguish species-level lineages of *Trebouxia* by including additional traits by means of new microscopy approaches.

High-end Scanning Electron Microscopy imaging of fully hydrated biological samples can be attained by cryo-fixing them freshly and maintaining the frozen condition in the SEM [31]. Thus, Low Temperature Scanning Electron Microscopy (LTSEM) arises as a powerful tool to obtain biological images with minimum intervention over the sample. LTSEM frequently includes additional freeze-fracture and freeze-etching steps, in which samples are mechanically sectioned and superficial water is removed by sublimation to reveal the underlying structures. For the past few decades, microalgae samples have been frozen and cryo-fractured to observe and analyse their morphology and ultrastructure. Detailed ultrastructure of microalgae [32,33], and in particular green microalgae [34–39], has been explored by LTSEM, yielding outstanding results. LTSEM of axenically cultured lichen phycobionts for cell ultrastructure has been performed only in *Asterochloris glomerata* [40]. Although LTSEM of in vitro cultured *Trebouxia* phycobionts has also been performed, only the cell morphology, cell wall, or extracellular substances have been analysed so far [8,13,41,42].

In order to find new morphological and ultrastructural traits with the potential to be added to the taxonomic discrimination of *Trebouxia* species in the future, here we explore the detailed ultrastructure of *T. lynnae* as observed by LTSEM. In addition, we reinterpreted the original TEM images of *T. lynnae*, as well as those of other *Trebouxia* species-level lineages, based on the new information provided by LTSEM.

2. Materials and Methods

2.1. Microalgae Strains and Growth Conditions

The analyses were performed on one strain of the lichen phycobiont *Trebouxia lynnae*. This strain was originally isolated from a thallus of *Ramalina farinacea* collected from the Sierra del Toro (39°57′ 32.34″ N–0°46′ 35.51″ W, Castellón, España). This microalga was both propagated several years by in vitro cultures and deposited and maintained as living culture at the "Symbiotic Algal collection from the University of Valencia" (ASUV, https://www.asuvalgae.com, accessed on 25 January 2023), and numbered as ASUV 44.

Microalgae strains maintained in the ASUV collection have been molecularly identified and are routinely monitored by means of ITS amplification and sequencing as described in Bordenave et al. [9]. *T. aggregata, T. anticipata T. arboricola, T. asymmetrica, T. australis, T. corticola*, *T. crenulata, T. crespoana, T. cretacea, T. decolorans, T. flava, T. gigantea, T. impressa, T. incrustata, T. jamesii, T. maresiae, T. potteri, T. showmanii,* and *T. simplex* were used for TEM analyses. Additional information about *Trebouxia* strains is available in the supplementary table (Supplementary Table S1). Microalgae strains were maintained axenically in Petri dishes on solid Bold's Basal Medium (BBM) [43,44] for 21 days in a growth chamber at 20 °C under a 12:12 h light:dark cycle (25 µmol photons m^{-2} s^{-1}). At 21 days, entire colonies were scraped from the substrate, resuspended in 3N liquid BBM solution (supplemented with glucose 20 g l^{-1} and casein 10 g l^{-1}), counted in Neubauer's chamber, and adjusted to 5.10^7 cells/µL. 50 µL of filtered cell suspension were applied directly over solid 3N BBM or over acetate discs deposited on the same medium. The Petri dishes were incubated in a growth chamber at 20 °C under a 12:12 h light:dark cycle (25 µmol photons m^{-2} s^{-1}).

2.2. Low Temperature Scanning Electron Microscopy (LTSEM)

For LTSEM, microalgal colonies plus the underlying agar medium or acetate discs were cut into squares of around 2 × 2 mm from the centre of the colony and attached to a cryo-holder using colloidal graphite. Samples were plunge frozen in LN2 slush and transferred with a transfer rod module into the cryo-preparation system (PP3010T, Quorum Technologies, Sussex, UK). Samples were mechanically freeze-fractured and then freeze-etched by sublimation for 15 to 25 min at −90 °C. The time of sublimation was adjusted to the estimated water content of the sample and the type of structures aimed at imaging. A thin layer of platinum was sputtered onto the specimens for 10 s and afterward transferred into a Field Emission Scanning Electron Microscope (FESEM ZEISS Ultra-55, Carl ZEISS SMT, Oberkochen, Germany). Images were recorded at an accelerating voltage of 1.5 kV. The images are photographic negatives; hence, protuberant elements of the fractured/etched surface are most heavily coated with platinum and appear white.

2.3. Transmission Electron Microscopy (TEM)

For TEM analyses, a portion of the sample of the microalgal colony of about 2 × 2 mm was covered with tempered low melting point agarose at 1%, fixed in Karnovsky fixative (with para-formaldehyde 2.5% and glutaraldehyde 0.5%) for 12 h at 4 °C, washed three times for 15 min with 0.01 M PBS (pH 7.4), and postfixed with 2% OsO_4 in 0.01 M PBS (pH 7.4) for 2 h at room temperature. After washing in 0.01 M PBS, pH 7.4, the samples were dehydrated at room temperature in a graded series of ethanol, starting at 50% and increasing to 70%, 95%, and 100% for at least 20–30 min at each step. The fixed and dehydrated samples were embedded in LR-White resin. Finally, increasing ethanol and resin infiltrations were carried out (two parts 90% ethanol plus one part resin, one part 90% ethanol plus two parts resin, and one part 100% ethanol plus two parts resin) until attaining 100% LR-White resin. Samples were then incubated at 60 °C for the resin to polymerizate. Ultra-thin sections, 60–90 nm thick, were cut with a UC7 Leica Ultramicrotome (Leica-Biosystems, Wetzlar, Germany) endowed with a diamond knife (Diatome ultra 458, Diatome, Switzerland), mounted on 100 mesh copper grids, and then stained with 10% uranyl acetate and Reynolds solution (0.1% lead citrate) using the 'Synaptek Grid-Stick Kit'. Sections were observed at 80 kV under a JEOL JEM-1010 microscope (Jeol, Peabody, MA, USA). Images were obtained using an Olympus MegaView III camera and processed with Fiji distribution of ImageJ [45].

3. Results and Discussion

3.1. General Aspects of Axenically Cultured Trebouxia lynnae LTSEM for Cell Ultrastructure Analysis

Most LTSEM protocols for microalgae were optimized for aquatic microalgae, which are axenically grown in liquid media [33–39]. Even when used with algae grown over solid media, the structure of the algal colony was not preserved [40]. *Trebouxia* microalgae, when

grown over solid media, proliferate in thick colonies around 1 mm tall [7,46]. Here, we used square-shaped samples of 2 × 2 mm, including the underlying agar, in order to maintain the original colony structure of the region to be analysed (Figure 1A). As a result, the surface of the samples is very irregular due to the differential cell growth (Figure 1B). Furthermore, it is possible to apply this approach to analyse different regions of the colony by selecting samples according to their distance from the center of the colony (Figure 1A). Acetate discs over the solid media were also used. In this case, the colony and the underlying disc were sectioned without taking the medium below.

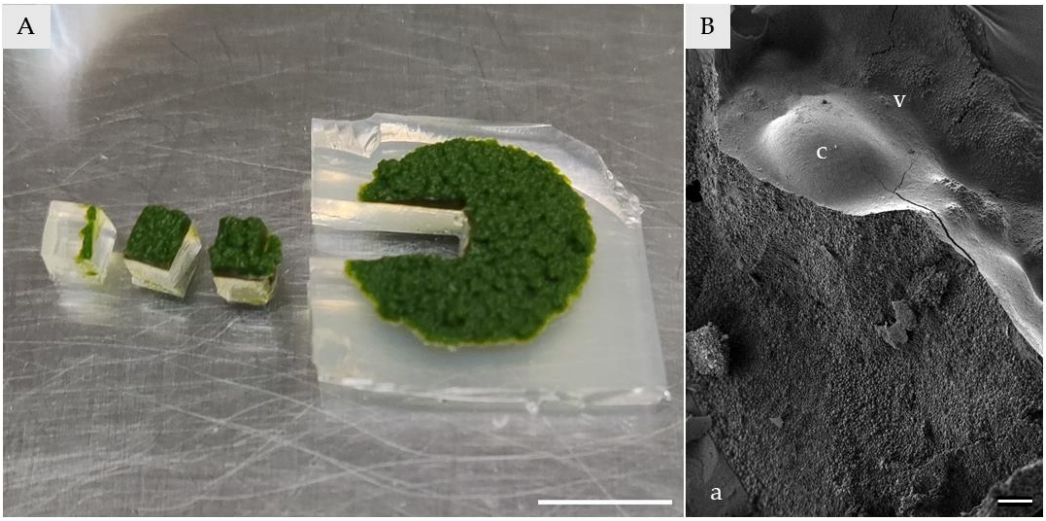

Figure 1. (**A**) Sample preparation before attaching to the cryo-holder: square-shaped samples of 2 × 2 mm of axenically cultured *Trebouxia lynnae* were cut, including the underlaying agar, in order to maintain the colony structure of the region to be analysed. (**B**) LTSEM of *T. lynnae*: general view of the cross-section of the colony, displaying the crests (c) and valleys (v) and the underlaying agar (a). Scale bar: (**A**) 100 µm, (**B**) 10 mm.

So far, no typical biological sample preparation procedure for LTSEM is available. When freeze-fracture coupled with freeze-etching is used for investigating the cell contents, the procedure can be divided into four main steps: first, the rapid freezing of the sample, second, the mechanical fracture, third, freeze etching by sublimation, and fourth, covering the surface with a spout to give contrast.

The rapid freezing of the sample has many alternatives [47], but plunging the sample in LN2 slush yielded good results for *Trebouxia*, and minimum to no water crystal formation was observed. The size of the sample was good for the following mechanical freeze-fracturing step, as just a small amount of debris remained over the fractured sample. On the contrary, freeze-etching by sublimation was unsuccessful under the most common conditions for microalgae LTSEM. Previous works with microalgae reported times of sublimation of 2 min [32,33,39,40] and 5 min [34,35,37]. Here, times as high as 20 min were needed to reveal the *Trebouxia* cell ultrastructure. Times of sublimation shorter than 15 min resulted in low contrast, the presence of ice, and an orange peel texture (Supplementary Figure S1). The high water content of the underlying agar was ruled out to be the cause of the high time of sublimation required, as the samples grown over the acetate disc also needed at least 15 min of sublimation. Lichen and its phycobionts are extremely tolerant to dehydration [42,48–53]. Recently, Bruñas et al. [54] obtained surprising results applying NIRS aquaphotomics to analyse *Ramalina farinacea* phycobionts. They demonstrated that *T. lynnae* allocates water molecules to high-bonding conformations. High-bounding waters require significantly higher times of sublimation than other conformations. Accumulation of cytoplasmic glycerol/polyol has been reported in *Trebouxia*. The sugar alcohols form hydration shells, which reduce water activity and impede water sublimation. Another explanation that cannot be discarded is that highly hydrated extra-

cellular substances that have an impact on the sublimation times may be present when working with sections of the thick colonies. Casano et al. [13] observed and analysed these extracellular substances both by LTSEM and biochemically, reporting the higher values of extracellular substances in *T. lynnae* among the assayed strains.

As expected from previous reports [9], no differences were observed between the growing conditions (solid medium vs. acetate discs laid over the solid medium, Supplementary Figure S2).

Within the *T. lynnae* colony, different types of cells were recognized both by LTSEM and by TEM. Young cells (6 ± 2 µm; Figure 2A,B) presented shallowly lobed chloroplasts displaying a low number of lobes and a single pyrenoid. Mature vegetative cells (10 ± 1 µm; Figure 2C,D) had shallowly lobed chloroplasts and a single impressa-type pyrenoid [9]. In both young and mature vegetative cells, a high number of vesicles was observed, and a moderate number of mitochondria could be distinguished, although they were inconspicuous. Mature vegetative cells displayed a big nucleus with a clearly distinguishable nucleolus.

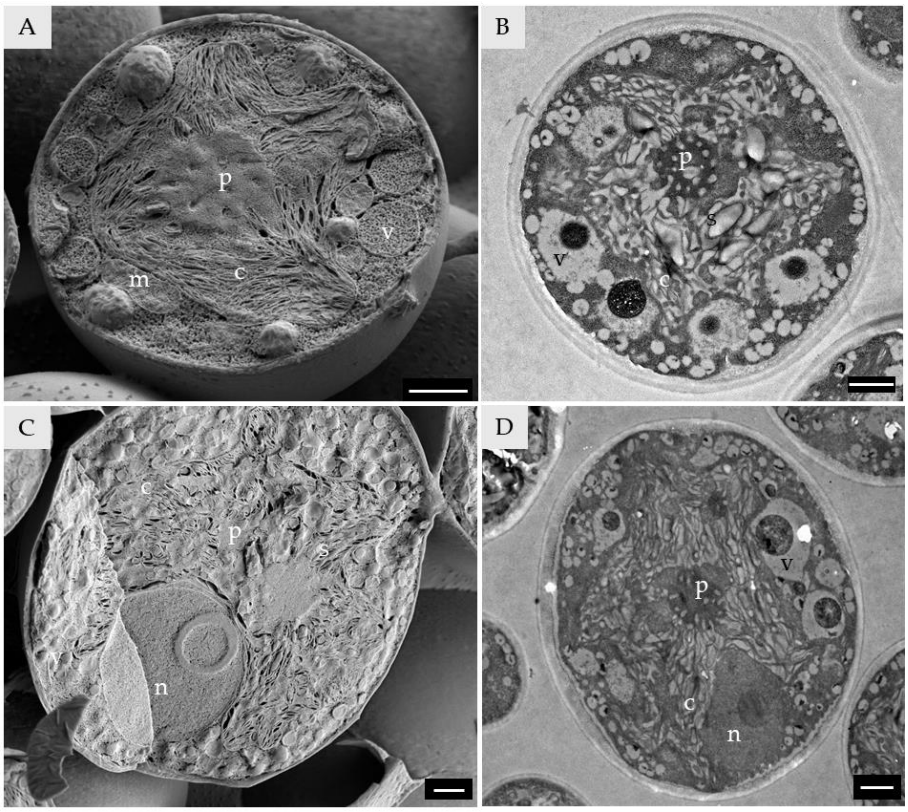

Figure 2. LTSEM (**A**,**C**) and TEM (**B**,**D**) of *Trebouxia lynnae* vegetative cells. (**A**,**B**) Young vegetative cells. (**C**,**D**) Mature vegetative cell. Chloroplast (c), pyrenoid (p), vesicles (v), starch grains (s), mitochondria (m), and nucleus (n) are indicated with letters. Scale bars: (**A**–**D**) 1 µm.

Two types of sporangia were observed (Figures 3 and 4). One in which spores with cell walls are symmetrically arranged (11–13 µm; Figure 3), presumably autosporangia (i.e., mitotic sporangia carrying cell-walled spores that resemble the morphology of vegetative cells). The chloroplast of the autospores was of the shallowly lobed type [9], with a low number of lobes (Figure 3A,B). The pyrenoid was recognizable as impressa-type (Figure 3A). Before opening, the spaces between cells are filled with an aqueous substance (Figure 3A,B) that is missing when the envelope is opened (Figure 3C). The autosporangia envelope was frequently persistent, even at the maturity of the daughter cells (Figure 3D,E).

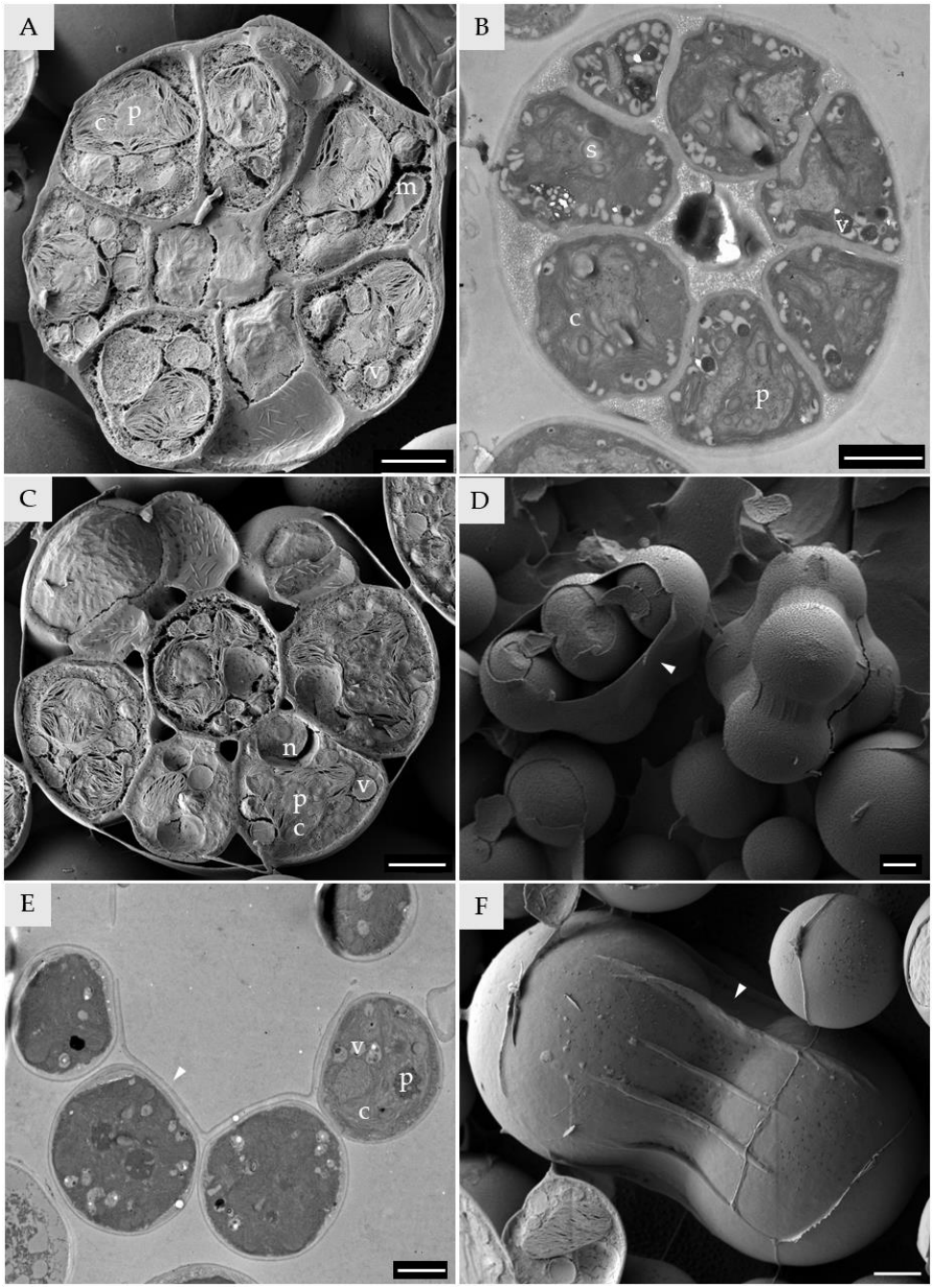

Figure 3. LTSEM (**A**,**C**,**D**,**F**) and TEM (**B**,**E**) of *Trebouxia lynnae* autosporangia. (**A**,**B**) Closed autosporangia. (**C**) Open autosporangia. (**D**,**E**,**F**) Vegetative cells inside the persistent autosporangium envelope. Chloroplast (c), pyrenoid (p), vesicles (v), starch grains (s), mitochondria (m), and nucleus (n) are indicated with letters. A persistent autosporangium envelope is indicated by a white arrowhead. Scale bars: (**A**–**F**) 2 µm.

The other sporangia contained naked spores that were asymmetrically arranged (Figure 4), presumably zoosporangia (i.e., sporangia carrying naked flagellated spores). Flagella were observed both by LTSEM (Figure 4A) and by TEM inside the zoosporangia (Figure 4B).

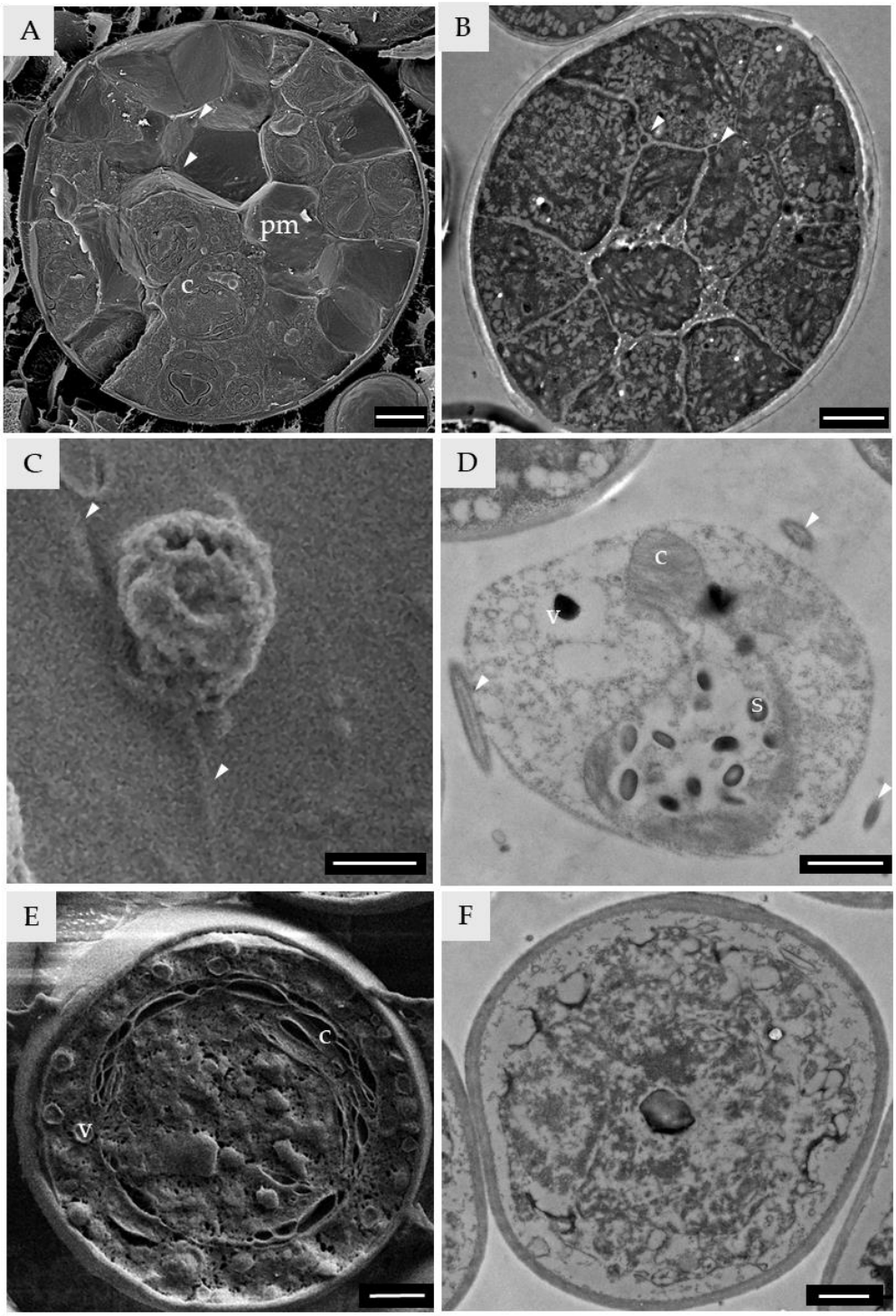

Figure 4. LTSEM (**A**,**C**,**E**) and TEM (**B**,**D**,**F**) of *Trebouxia lynnae* zoosporangia, zoospores, and senescent cells. (**A**,**B**) Zoosporangia. (**C**,**D**) Zoospores. (**E**,**F**) Senescent cells. Chloroplast (c), vesicles (v), starch grains (s), and plasma membrane (pm) are indicated with letters. Flagella are indicated by a white arrowhead. Scale bars: (**A**,**B**) 2 µm, (**C**–**F**) 1 µm.

Flagellated cells (around 7 µm; Figure 4), presumably zoospores (i.e., naked flagellated spores), are fragile and usually suffer from cytolysis. Zoospores were observed by LTSEM (Figure 4C) and TEM (Figure 4D), always showing the complete absence of the cell wall. Chloroplasts were shallowly lobed with abundant starch grains (Figure 4D).

Finally, cells bearing a parietal chloroplast with a central cavity, presumably senescent cells, were observed both in LTSEM (Figure 4E) and TEM (Figure 4F).

3.2. Chloroplast and Pyrenoid

T. lynnae presents a single massive, axial chloroplast with a shallowly lobed morphology, as reported previously (Figures 2 and 5) [8,9]. The surface of the chloroplast depicted shallow lobes to which the thylakoids project from the centre of the chloroplast (Figure 5A,B,E). A chloroplast pocket is always present where the nucleus is located, tightly embraced by the chloroplast (Figure 5C,D). Each chloroplast usually displays a single pyrenoid, although multiple pyrenoids per cell were occasionally observed. *T. lynnae* pyrenoids belong to the impressa-type, as previously reported [8,9]. These pyrenoids are characterized by radial, straight, unbranched tubules penetrating the pyrenoid matrix, appearing either long or short depending on the orientation of the section, with the pyrenoid matrix thicker than the tubules. LTSEM allowed to clearly distinguish the thylakoid lamellae from which the pyrenotubules originates (Figure 5F).

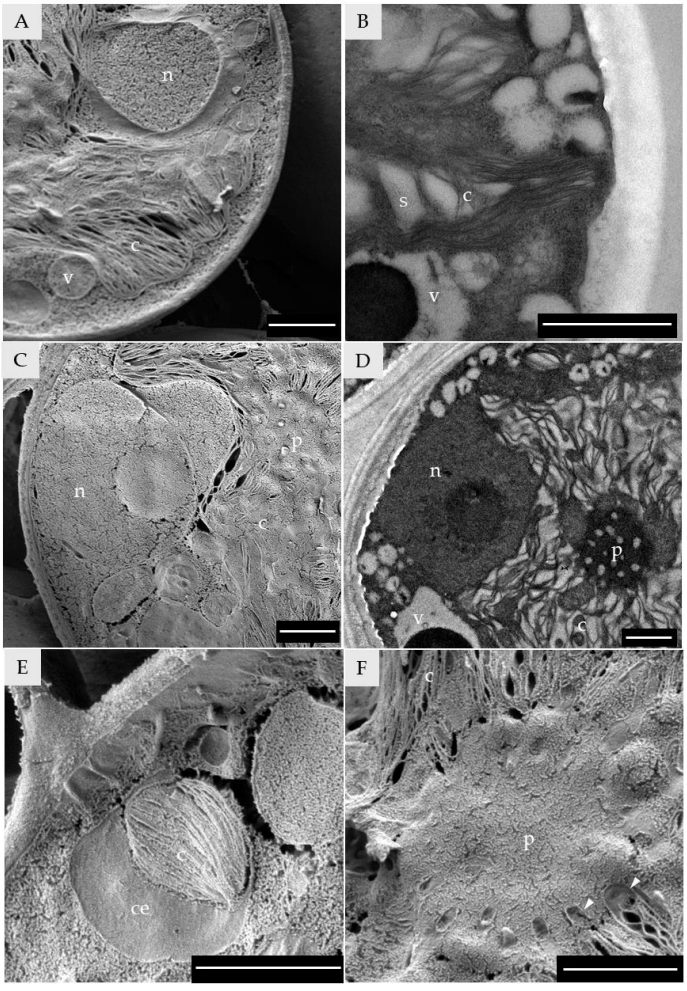

Figure 5. LTSEM (**A**,**C**,**E**,**F**) and TEM (**B**,**D**) of *Trebouxia lynnae* chloroplasts. (**A**,**B**) Chloroplast shallow lobes. (**C**,**D**) Chloroplast pockets. (**E**) Chloroplast lobule. (**F**) Pyrenoid. Chloroplast (c), chloroplast envelope (ce), nucleus (n), starch granules (s), vesicles (v), and pyrenoid (p) are indicated with letters. Thylakoid lamellae transitioning into pyrenotubules are indicated by a white arrowhead. Scale bars: (**A**–**F**) 1 µm.

3.3. Nucleus

Vegetative cells of *T. lynnae* present a round nucleus, occupying a significant fraction of the cell volume (Figure 2C,D). The nucleus is always located in the chloroplast

pocket (Figures 5C,D and 6A,B). When the freeze-fracture revealed the nuclear envelope surface, nuclear pores were distinguishable with a regular distribution (Figure 6A). Material deposited in the nuclear pores was observed, presumably proteins or protein complexes translocating through the nuclear pores (Figure 6A). When the nucleus was sectioned by the freeze-fracture, both membranes of the nuclear envelope could be observed (Figure 6C–E). The nuclei of vegetative cells usually display a nucleolus (Figures 2C,D, 5C,D and 6C–F). LTSEM revealed that the nucleolus of *T. lynnae* mature vegetative cells frequently possessed a central nucleolar vacuole (Figure 6C,E). Although nucleolar vacuole function is still discussed [55], it is thought that in plants it indicates a highly active nucleus [56]. Being aware of this feature of LTSEM, it was possible to identify the nucleolar vacuole in samples of *T. lynnae* observed with TEM (Figure 6F). Furthermore, the nucleolar vacuole was observed in cells of 61% of the *Trebouxia* species-level lineages analysed (Supplementary Figure S3).

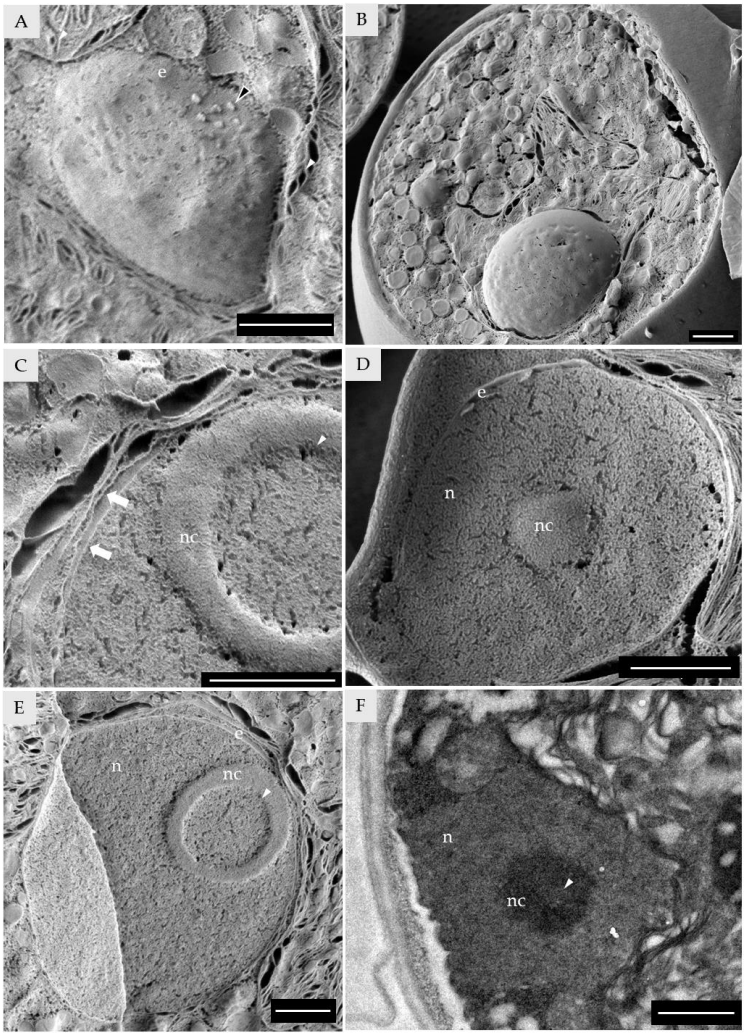

Figure 6. LTSEM (**A**–**E**) and TEM (F) of *Trebouxia lynnae* nuclei. (**A**) Surface of a whole nucleus. (**B**) Nucleus inside the chloroplast pocket. (**C**) Double membrane of the nuclear envelope of a fractured nucleus. (**D**) Fractured nucleus with a whole nucleolus. (**E**,**F**) Nucleus with a fractured (sectioned) nucleolus with a nucleolar vacuole. Nucleus (n), nucleolus (nc), and nuclear envelope (e) are indicated with letters. The nucleolar vacuole is indicated by a white arrowhead. Material that accumulates at the surface of the nuclear pore is indicated by a black arrowhead. Inner and outer membranes of the nuclear envelope are indicated by white arrows. Scale bars: (**A**–**F**) 1 μm.

The observation of the nuclear pores and both membranes of the nuclear envelope is facilitated by LTSEM, whereas it is difficult, if not impossible, to achieve by standard TEM procedures. In addition, LTSEM allowed the observation of the nucleolar vacuole and its identification in TEM images of *T. lynnae* and other *Trebouxia* species, making this one of the few reports of nucleolar vacuoles in microalgae [57].

3.4. Cytosol and Cytosolic Organelles

The cytosol of *T. lynnae* was revealed to be a highly crowded compartment, with a large amount of globular structures populating it. There were also a variety of membranous structures, vesicles, and droplets, evident either by LTSEM or TEM observation (Figure 7).

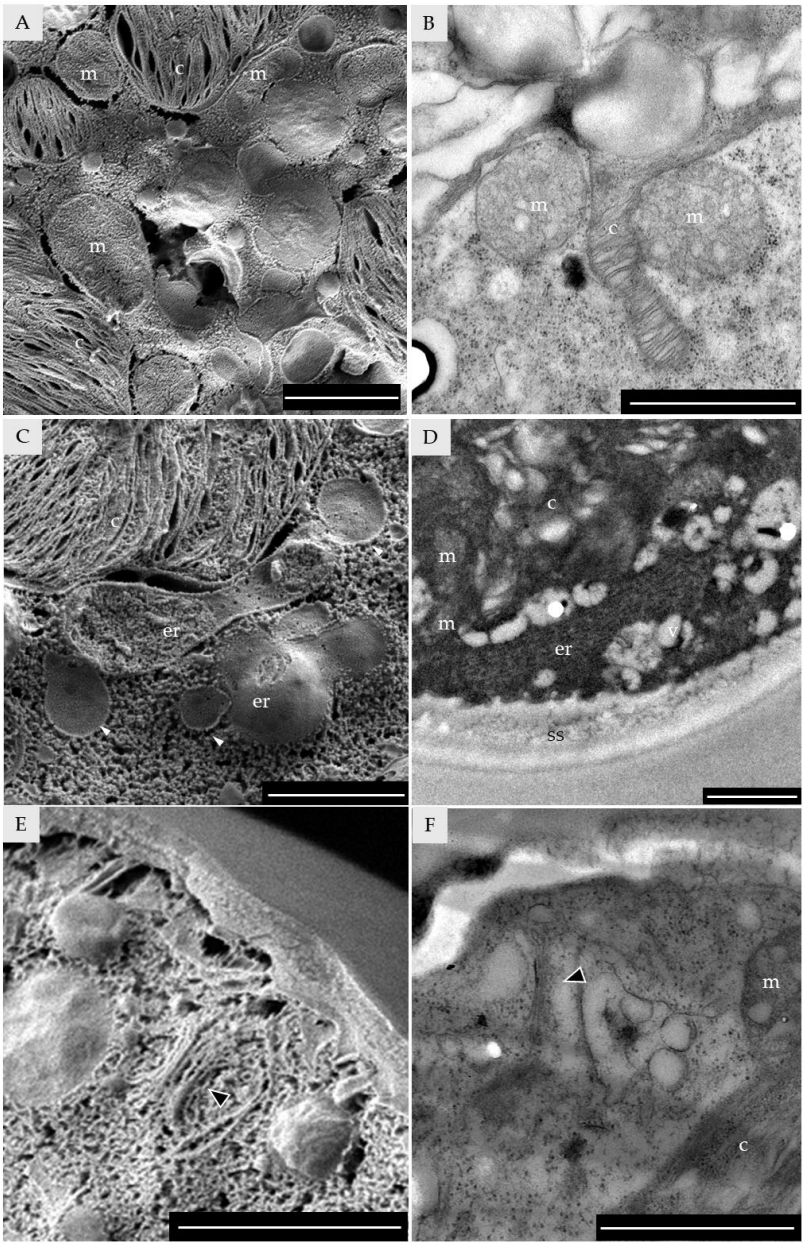

Figure 7. LTSEM (**A**,**C**,**E**) and TEM (**B**,**D**,**F**) of *Trebouxia lynnae* mitochondria and secretion system. (**A**,**B**) Mitochondria. (**C**,**D**) Fenestrated endoplasmic reticulum. (**E**,**F**) Dictyosome. Mitochondria (m), endoplasmic reticulum (er), secretion space (ss), and chloroplast (c) are indicated with letters. The dictyosome is indicated by a black arrowhead. Endoplasmic reticulum trafficking vesicles are indicated by white arrowheads. Scale bars: (**A**–**F**) 1 µm.

Mitochondria were observed in high numbers in LTSEM (Figure 7), although their internal structures were difficult to discern (Figure 7A,B). TEM images allowed us to observe the internal structures of the mitochondria in *T. lynnae* (Figure 7C), as already reported by Casano et al. [12]. As expected, every *Trebouxia* species-level lineage analysed by TEM presented well-developed mitochondria (Supplementary Figure S4). The overall ultrastructure of *Trebouxia* mitochondria was similar to that of mitochondria observed in other *Trebouxiophyceae* algae [58,59]. For each *Trebouxia* analysed here, a wide range of shapes and sizes was observed, even within the same cell (Supplementary Figure S4). This was already reported decades ago in some species of microalgae [59]. In several species of the *Chlorella* genus, it has been demonstrated that each cell contains a single, tubular, branched mitochondrion [60–62].

The diversity of morphologies observed in our results indicates that *Trebouxia* may also have tubularly branched mitochondria. To assert the number of this organelle present in each cell of these microalgae, other microscopy approaches may be needed.

Guo et al. [62] reported that the chloroplast and mitochondrial membranes of *Chlorella pyrenoidosa* run parallel to each other, hypothesizing that there may exist a mechanism of direct translocation of NADPH and ATP between these compartments in these microalgae. In *T. lynnae* (Figure 7B), as well as other *Trebouxia* species-level lineages (Supplementary Figure S4), a close proximity between the membranes of these two compartments is observed. How this phenomenon affects the efficiency of the *Trebouxia* metabolism compared to other microalgae and plants having different mitochondria/chloroplast architectures is still unknown.

Endoplasmic reticulum and dictyosomes are inconspicuous in *T. lynnae*, probably due to the cytosol crowding in cells with a low ratio of cytosol/chloroplast volumes, and have never been reported by TEM ultrastructure analyses before. Here, LTSEM allowed for the identification of both organelles (Figure 7C–F). Endoplasmic reticulum was observed as a fenestrated system of cisternae from which trafficking vesicles sprout (Figure 7C,D), similar to those observed in *Botryococcus braunii* [39]. Dictyosomes were observed as a group of flattened cisternae of around 0.2 × 0.5 µm (Figure 7E,F). In TEM images, we were able to recognise the endoplasmic reticulum as a stack of membranous structures with a punctuated electrodense texture, likely ribosomes (Figure 7D). Endoplasmic reticulum was frequently located at the periphery of the cell, next to the widest section of the secretion space (Figure 7D and Supplementary Figure S5).

Both endoplasmic reticulum and dictyosomes were observed in around 28% of other *Trebouxia* species-level lineages (Supplementary Figures S5 and S6).

Vesicles and droplets were distinguishable from each other by the presence or absence of a membrane, respectively (Figure 8A–C). However, droplets inside some vesicles were also observed (Figure 8B,C). Multivesicular bodies, highly packaged vesicles inside a membranous structure, were also identified (Figure 8D). Multivesicular bodies have been reported to facilitate the trafficking of a variety of cargo through both the cell membrane and the cell wall [63].

The amount and diversity of vesicles, including multivesicular bodies, the presence of well-developed fenestrated endoplasmic reticulum and dictyosomes, and the location of the secretion system in the vicinity of the secretion space suggest that *T. lynnae* is secreting high amounts of extracellular substances, as already observed in other *Trebouxiales* [39]. This is also in line with the results reported by González-Hourcade et al. [42,53] on the extracellular polysaccharides and proteins of *T. lynnae*.

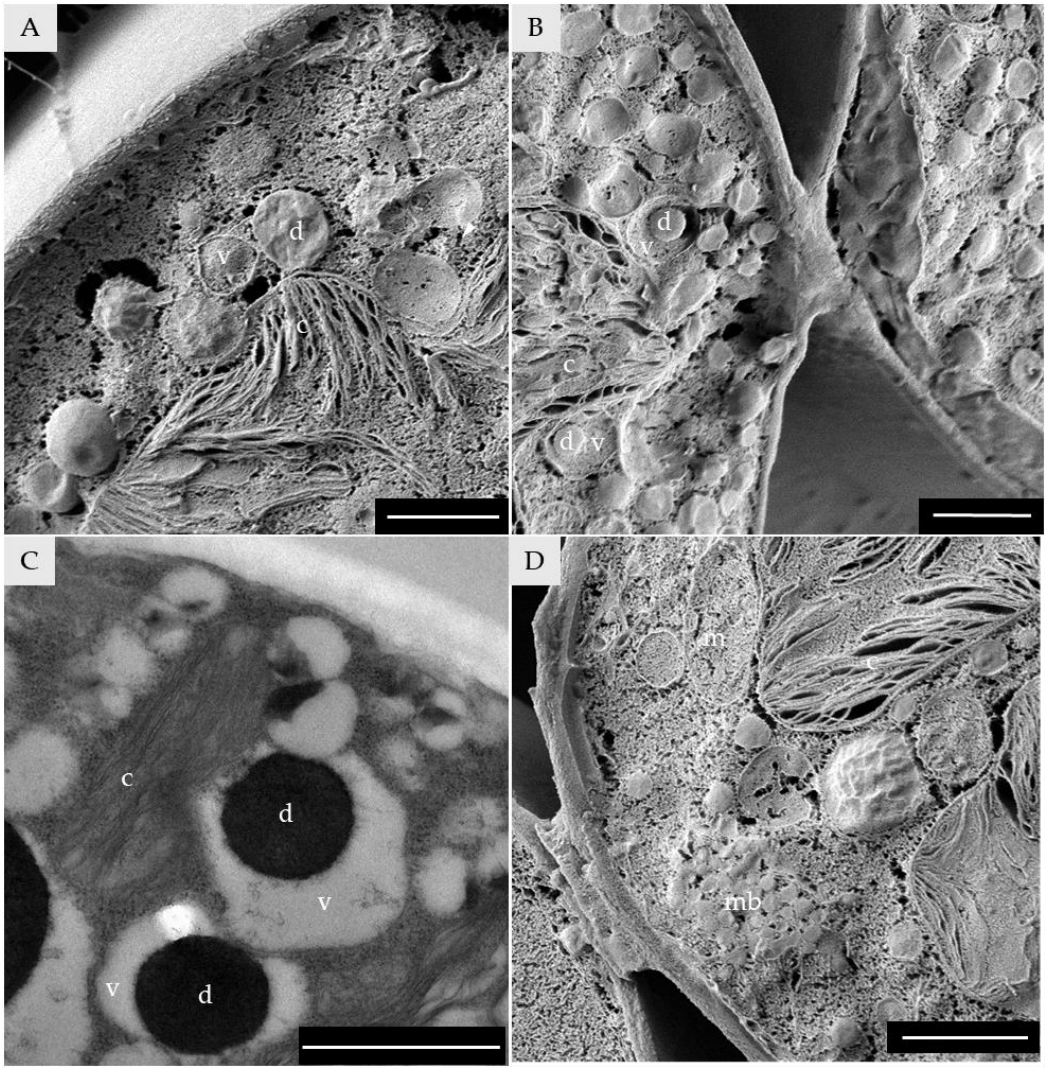

Figure 8. LTSEM (**A**,**B**,**D**) and TEM (**C**) of *Trebouxia lynnae* vesicles. (**A**) Vesicles and lipid droplets. (**B**,**C**) Lipid droplets inside vesicles. (**D**) Multivesicular body. Chloroplast (c), vesicles (v), lipid droplets (d), multivesicular bodies (mb), and mitochondria (m) are indicated with letters. Scale bars: (**A**–**D**) 1 µm.

3.5. Cell-Wall

T. lynnae cell wall was thick (0.25 ± 0.05 µm) and composed of at least three layers (Figure 9B,C). Different layers of the cell wall were already reported for *T. lynnae* [8,12,42] and are also visible in TEM micrographs (Figure 9C). The cell wall of microalgae that contains a high amount of algaenan (sporopollenin) appears greasy/gummy when observed in LTSEM [33,40]. None of *T. lynnae* cell wall layers appeared greasy/gummy. This is in line with the observations of Gonzales-Hourcade et al. [42], in which the degree of crystal violet permeability in *T. lynnae* indicated the absence of this biopolymer in its cell wall. LTSEM images revealed some features of the *T. lynnae* cell-wall that are not evident with other microscopy approaches. The cell wall presents pores or cavities that seem to meander through the interior of the structure (Figure 9B). LTSEM (Figure 9A,B) and TEM (Figure 9D) also revealed the presence of fibers, either on the surface or as part of the cell wall structure. Fibre-like structures have been observed previously in the cell walls of the *Trebouxia* phycobiont of *Cladonia macrophylla* [64] and also in the phycobiont *Asterochloris glomerata* [40]. The porosity of the cell wall and the presence of fibre-like structures on its surface are also in line with the hypothesis of an important traffic between the intracellular compartments and the extracellular space.

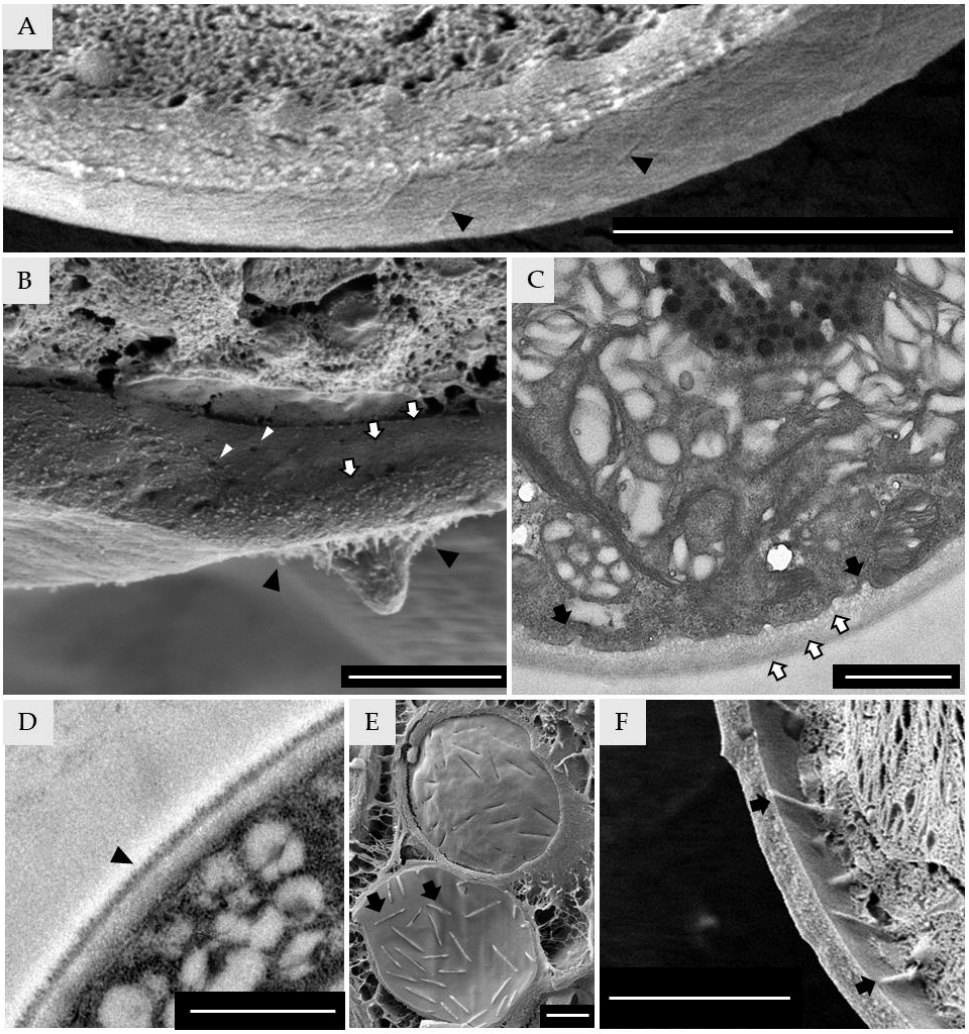

Figure 9. LTSEM (**A**,**B**,**E**,**F**) and TEM (**C**,**D**) of *Trebouxia lynnae* cell wall. (**A**) Cell wall depicting superficial fibers. (**B**,**C**) Cell wall depicting three layers, inner pores, and fibrils. (**D**) Fibrils on the surface of the cell wall. (**E**,**F**) Eisosomes. Cell wall layers are indicated by white arrows. Eisosomes are indicated by black arrows. Inner pores are indicated by white arrow heads. Fibrils are indicated by black arrowheads. Scale bars: (**A**–**F**) 1 µm.

When the inner face of the cell wall or the outer face of the cell membrane is exposed, regularly distributed, elongated eisosomes are visible (Figure 9C–F). Eisosomes are trough-shaped invaginations of the plasma membrane in which protein complexes nest and project up to the cell wall [41]. Eisosomes in the *Trebouxia* genus have been largely observed and described [40–42,65] and, although inconspicuous, can also be detected by TEM (Figure 9C).

4. Conclusions

LTSEM of *Trebouxia* phycobionts is presented here as a suitable method to expand the analysis of morphological and ultrastructural traits in lichen phycobionts. This technique contributes to reinterpreting how microalgal cell structures and compartments are shaped, and the results can be used to implement the taxonomic classification of lichen phycobionts in general. In addition, it allowed for the identification of elusive organelles and cell constituents that are difficult to observe by traditional microscopy approaches due to the nature of the procedures (steps of dehydration of the sample or affinity for the dyes for different structures) or the sample itself (high levels of cytosol crowding). Once the elusive structures are identified, it is possible to track them back with traditional microscopy for everyday benchwork, revaluing traditional microscopy methodologies, like TEM.

Our results are consistent with cell features, besides the chloroplast and the pyrenoid, and may be used for an integrative taxonomy of molecular and ultrastructural data in *Trebouxia* phycobionts.

LTSEM proves to be a methodology that uses a minimum amount of intervention on the biological sample. Applying LTSEM to *Trebouxia* phycobionts opens the door to analysing and observing microalgae samples as similar as possible to their intact condition. This will be highly desirable to assess the physiological and morphological state of phycobionts in axenic cultures or in the lichenized state, subjected to abiotic conditions such as desiccation, UV light, and salinity stresses, among many others.

Supplementary Materials: The following supporting information can be downloaded at: https://www.mdpi.com/article/10.3390/d15020170/s1, Figure S1: "Orange peel" artefact produced by a short time of sublimation; Figure S2: General ultrastructure of *Trebouxia lynnae* vegetative cells growing over different substrates; Figure S3: TEM micrographs showing the presence or absence of the nucleolar vacuole on *Trebouxia* species-level lineages; Figure S4: TEM micrographs showing mitochondrial morphology on *Trebouxia* species-level lineages; Figure S5: TEM micrographs of *Trebouxia* species-level lineages in which the endoplasmic reticulum was found; Figure S6: TEM micrographs of *Trebouxia* species-level lineages in which the dictyosome was found; Table S1: list of *Trebouxia* species-level lineages used in the TEM analysis with their isolation information.

Author Contributions: Conceptualization, C.D.B., F.G.-B., E.B. and L.M.; methodology, F.G.-B., C.D.B. and E.B.; formal analysis, C.D.B., F.G.-B. and E.B.; investigation, C.D.B., F.G.-B., E.B. and A.G.; resources, E.B., F.G.-B., writing—original draft preparation, C.D.B., A.G.; writing—review and editing, C.D.B., F.G.-B., E.B., A.G., L.M. and P.C.; visualization, C.D.B.; supervision, F.G.-B., E.B., L.M. and P.C.; project administration, E.B. and P.C.; funding acquisition, E.B. and P.C. All authors have read and agreed to the published version of the manuscript.

Funding: Funding for this study was provided by the PROMETEO Excellence in Research Program (PROMETEO/2021/005, Generalitat Valenciana, Spain) and Grant PID2021-127087NB-100 funded by MCIN/AEI/10.13039/501100011033. Bordenave, CD, received funding from a postdoctoral grant of the Generalitat Valenciana and the European Social Fund (APOSTD19) and the María Zambrano from the Ministerio de Universidades (grant ZA21-046). Gázquez, A. received funding from a postdoctoral grant of the Generalitat Valenciana and the European Social Fund (APOSTD21).

Institutional Review Board Statement: Not applicable.

Data Availability Statement: The data presented in this study is contained within the article or supplementary material.

Acknowledgments: We thank all the staff of the microscopy section of the SCSIE Burjassot-Paterna and of the Electron Microscopy Service from the Universitat Politècnica de València.

Conflicts of Interest: The authors declare no conflict of interest.

References

1. Hawksworth, D.L.; Grube, M. Lichens redefined as complex ecosystems. *New Phytol.* **2020**, *227*, 1281–1283. [CrossRef] [PubMed]
2. Friedl, T. Systematik und biologie von *Trebouxia* (Microthamniales, Chlorophyta) als phycobiont der *Parmeliaceae* (lichenisierte Ascomyceten). Ph.D. Thesis, Universitat Bayreuth, Bayreuth, Germany, 1989.
3. Tschermak-Woess, E. The Algal Partner. In *Handbook of Lichenology*; CRC Press: Boca Raton, FL, USA, 2019; pp. 39–92, ISBN 0429291787.
4. Friedl, T. Comparative ultrastructure of pyrenoids in *Trebouxia* (Microthamniales, Chlorophyta). *Plant Syst. Evol.* **1989**, *164*, 145–159. [CrossRef]
5. Muggia, L.; Leavitt, S.; Barreno, E. The hidden diversity of lichenised *Trebouxiophyceae* (Chlorophyta). *Phycologia* **2018**, *57*, 503–524. [CrossRef]
6. Leavitt, S.D.; Kraichak, E.; Nelsen, M.P.; Altermann, S.; Divakar, P.K.; Alors, D.; Esslinger, T.L.; Crespo, A.; Lumbsch, T. Fungal specificity and selectivity for algae play a major role in determining lichen partnerships across diverse ecogeographic regions in the lichen-forming family *Parmeliaceae* (Ascomycota). *Mol. Ecol.* **2015**, *24*, 3779–3797. [CrossRef] [PubMed]
7. Muggia, L.; Nelsen, M.P.; Kirika, P.M.; Barreno, E.; Beck, A.; Lindgren, H.; Lumbsch, H.T.; Leavitt, S.D. Formally described species woefully underrepresent phylogenetic diversity in the common lichen photobiont genus *Trebouxia* (Trebouxiophyceae, Chlorophyta): An impetus for developing an integrated taxonomy. *Mol. Phylogenet. Evol.* **2020**, *149*, 106821. [CrossRef]

8. Barreno, E.; Muggia, L.; Chiva, S.; Molins, A.; Bordenave, C.; García-Breijo, F.; Moya, P. *Trebouxia lynnae* sp. nov. (former *Trebouxia* sp. TR9): Biology and biogeography of an epitome lichen symbiotic microalga. *Biology* **2022**, *11*, 1196. [CrossRef]
9. Bordenave, C.D.; Muggia, L.; Chiva, S.; Leavitt, S.D.; Carrasco, P.; Barreno, E. Chloroplast morphology and pyrenoid ultrastructural analyses reappraise the diversity of the lichen phycobiont genus *Trebouxia* (Chlorophyta). *Algal. Res.* **2022**, *61*, 102561. [CrossRef]
10. Hinojosa-Vidal, E.; Marco, F.; Martínez-Alberola, F.; Escaray, F.J.; García-Breijo, F.J.; Reig-Armiñana, J.; Carrasco, P.; Barreno, E. Characterization of the responses to saline stress in the symbiotic green microalga *Trebouxia* sp. TR9. *Planta* **2018**, *248*, 1473–1486. [CrossRef]
11. del Hoyo, A.; Álvarez, R.; del Campo, E.M.; Gasulla, F.; Barreno, E.; Casano, L.M. Oxidative stress induces distinct physiological responses in the two Trebouxia phycobionts of the lichen *Ramalina farinacea*. *Ann. Bot.* **2011**, *107*, 109–118. [CrossRef]
12. Casano, L.M.; del Campo, E.M.; García-Breijo, F.J.; Reig-Armiñana, J.; Gasulla, F.; del Hoyo, A.; Guéra, A.; Barreno, E. Two *Trebouxia* algae with different physiological performances are ever-present in lichen thalli of *Ramalina farinacea*. Coexistence versus competition? *Environ. Microbiol.* **2011**, *13*, 806–818. [CrossRef]
13. Casano, L.M.; Braga, M.R.; Álvarez, R.; del Campo, E.M.; Barreno, E. Differences in the cell walls and extracellular polymers of the two *Trebouxia* microalgae coexisting in the lichen *Ramalina farinacea* are consistent with their distinct capacity to immobilize extracellular Pb. *Plant Sci.* **2015**, *236*, 195–204. [CrossRef]
14. Martínez-Alberola, F.; Barreno, E.; Casano, L.M.; Gasulla, F.; Molins, A.; del Campo, E.M. Dynamic evolution of mitochondrial genomes in *Trebouxiophyceae*, including the first completely assembled mtDNA from a lichen-symbiont microalga (*Trebouxia* sp. TR9). *Sci. Rep.* **2019**, *9*, 8209. [CrossRef]
15. Martínez-Alberola, F.; Barreno, E.; Casano, L.M.; Gasulla, F.; Molins, A.; Moya, P.; González-Hourcade, M.; Campo, E.M. The chloroplast genome of the lichen-symbiont microalga *Trebouxia* sp. Tr9 (*Trebouxiophyceae*, Chlorophyta) shows short inverted repeats with a single gene and loss of the rps4 gene, which is encoded by the nucleus. *J. Phycol.* **2020**, *56*, 170–184. [CrossRef]
16. Nelsen, M.P.; Leavitt, S.D.; Heller, K.; Muggia, L.; Lumbsch, H.T. Contrasting patterns of climatic niche divergence in *Trebouxia*—A clade of lichen-forming algae. *Front. Microbiol.* **2022**, *13*, 791546. [CrossRef]
17. Molins, A.; Moya, P.; García-Breijo, F.J.; Reig-Armiñana, J.; Barreno, E. Molecular and morphological diversity of *Trebouxia* microalgae in sphaerothallioid *Circinaria* spp. lichens. *J. Phycol.* **2018**, *54*, 494–504. [CrossRef]
18. Dal Grande, F.; Rolshausen, G.; Divakar, P.K.; Crespo, A.; Otte, J.; Schleuning, M.; Schmitt, I. Environment and host identity structure communities of green algal symbionts in lichens. *New Phytol.* **2018**, *217*, 277–289. [CrossRef]
19. Molins, A.; Moya, P.; Muggia, L.; Barreno, E. Thallus growth stage and geographic origin shape microalgal diversity in *Ramalina farinacea* lichen holobionts. *J. Phycol.* **2021**, *57*, 975–987. [CrossRef]
20. Moya, P.; Molins, A.; Škaloud, P.; Divakar, P.K.; Chiva, S.; Dumitru, C.; Molina, M.C.; Crespo, A.; Barreno, E. Biodiversity patterns and ecological preferences of the photobionts associated with the lichen-forming genus *Parmelia*. *Front. Microbiol.* **2021**, *12*, 3950. [CrossRef]
21. Moya, P.; Chiva, S.; Molins, A.; Garrido-Benavent, I.; Barreno, E. Unravelling the symbiotic microalgal diversity in *Buellia zoharyi* (lichenized Ascomycota) from the Iberian Peninsula and Balearic Islands using dna metabarcoding. *Diversity* **2021**, *13*, 220. [CrossRef]
22. Moya, P.; Molins, A.; Chiva, S.; Bastida, J.; Barreno, E. Symbiotic microalgal diversity within lichenicolous lichens and crustose hosts on Iberian Peninsula gypsum biocrusts. *Sci. Rep.* **2020**, *10*, 14060. [CrossRef]
23. Catalá, S.; del Campo, E.M.; Barreno, E.; García-Breijo, F.J.; Reig-Armiñana, J.; Casano, L.M. Coordinated ultrastructural and phylogenomic analyses shed light on the hidden phycobiont diversity of *Trebouxia* microalgae in *Ramalina fraxinea*. *Mol. Phylogenet. Evol.* **2016**, *94*, 765–777. [CrossRef] [PubMed]
24. Moya, P.; Molins, A.; Martínez-Alberola, F.; Muggia, L.; Barreno, E. Unexpected associated microalgal diversity in the lichen *Ramalina farinacea* is uncovered by pyrosequencing analyses. *PLoS ONE* **2017**, *12*, e0175091. [CrossRef] [PubMed]
25. Škaloud, P.; Moya, P.; Molins, A.; Peksa, O.; Santos-Guerra, A.; Barreno, E. Untangling the hidden intrathalline microalgal diversity in *Parmotrema pseudotinctorum*: *Trebouxia crespoana* sp. nov. *Lichenologist* **2018**, *50*, 357–369. [CrossRef]
26. Molins, A.; Chiva, S.; Calatayud, Á.; Marco, F.; García-Breijo, F.; Reig-Armiñana, J.; Carrasco, P.; Moya, P. Multidisciplinary approach to describe *Trebouxia* diversity within lichenized fungi *Buellia zoharyi* from the Canary Islands. *Symbiosis* **2020**, *82*, 19–34. [CrossRef]
27. Molins, A.; Moya, P.; García-Breijo, F.J.; Reig-Armiñana, J.; Barreno, E. Assessing lichen microalgal diversity by a multi-tool approach: Isolation, Sanger sequencing, HTS and ultrastructural correlations. *Lichenologist* **2018**, *50*, 123–138. [CrossRef]
28. Chiva, S.; Garrido-Benavent, I.; Moya, P.; Molins, A.; Barreno, E. How did terricolous fungi originate in the Mediterranean region? A case study with a gypsicolous lichenized species. *J. Biogeogr.* **2019**, *46*, 515–525. [CrossRef]
29. Moya, P.; Škaloud, P.; Chiva, S.; García-Breijo, F.J.; Reig-Armiñana, J.; Vančurová, L.; Barreno, E. Molecular phylogeny and ultrastructure of the lichen microalga *Asterochloris mediterranea* sp. nov. from mediterranean and Canary Islands ecosystems. *Int. J. Syst. Evol. Microbiol.* **2015**, *65*, 1838–1854. [CrossRef]
30. Garrido-Benavent, I.; Chiva, S.; Bordenave, C.D.; Molins, A.; Barreno, E. *Trebouxia maresiae* sp. nov. (*Trebouxiophyceae*, Chlorophyta), a new lichenized species of microalga found in coastal environments. *Cryptogam. Algol.* **2022**, *43*, 135–145. [CrossRef]
31. Schatten, H. *Scanning Electron Microscopy for the Life Sciences*; Cambridge University Press: Cambridge, UK, 2012; ISBN 1139851055.

32. Wolf, B.M.; Niedzwiedzki, D.M.; Magdaong, N.C.M.; Roth, R.; Goodenough, U.; Blankenship, R.E. Characterization of a newly isolated freshwater Eustigmatophyte alga capable of utilizing far-red light as its sole light source. *Photosynth. Res.* **2018**, *135*, 177–189. [CrossRef]
33. Scholz, M.J.; Weiss, T.L.; Jinkerson, R.E.; Jing, J.; Roth, R.; Goodenough, U.; Posewitz, M.C.; Gerken, H.G. Ultrastructure and composition of the *Nannochloropsis gaditana* cell wall. *Eukaryot. Cell* **2014**, *13*, 1450–1464. [CrossRef]
34. Peled, E.; Pick, U.; Zarka, A.; Shimoni, E.; Leu, S.; Boussiba, S. Light-induced oil globule migration in *Haematococcus pluvialis* (chlorophyceae). *J. Phycol.* **2012**, *48*, 1209–1219. [CrossRef]
35. Mulders, K.J.M.; Weesepoel, Y.; Bodenes, P.; Lamers, P.P.; Vincken, J.P.; Martens, D.E.; Gruppen, H.; Wijffels, R.H. Nitrogen-depleted *Chlorella zofingiensis* produces astaxanthin, ketolutein and their fatty acid esters: A carotenoid metabolism study. *J. Appl. Phycol.* **2015**, *27*, 125–140. [CrossRef]
36. Polle, J.E.W.; Roth, R.; Ben-Amotz, A.; Goodenough, U. Ultrastructure of the green alga *Dunaliella salina* strain CCAP19/18 (Chlorophyta) as investigated by quick-freeze deep-etch electron microscopy. *Algal. Res.* **2020**, *49*, 101953. [CrossRef]
37. Davidi, L.; Shimoni, E.; Khozin-Goldberg, I.; Zamir, A.; Pick, U. Origin of β-carotene-rich plastoglobuli in *Dunaliella bardawil*. *Plant Physiol.* **2014**, *164*, 2139–2156. [CrossRef]
38. Lamers, P.P.; van de Laak, C.C.W.; Kaasenbrood, P.S.; Lorier, J.; Janssen, M.; de Vos, R.C.H.; Bino, R.J.; Wijffels, R.H. Carotenoid and fatty acid metabolism in light-stressed *Dunaliella salina*. *Biotechnol. Bioeng.* **2010**, *106*, 638–648. [CrossRef]
39. Weiss, T.L.; Roth, R.; Goodson, C.; Vitha, S.; Black, I.; Azadi, P.; Rusch, J.; Holzenburg, A.; Devarenne, T.P.; Goodenough, U. Colony organization in the green alga *Botryococcus braunii* (Race B) is specified by a complex extracellular matrix. *Eukaryot. Cell* **2012**, *11*, 1424–1440. [CrossRef]
40. Roth, R.; Goodenough, U. Lichen 1. Solo fungal and algal partners. *Algal. Res.* **2021**, *58*, 102334. [CrossRef]
41. Lee, J.H.; Heuser, J.E.; Roth, R.; Goodenough, U. Eisosome ultrastructure and evolution in fungi, microalgae, and lichens. *Eukaryot. Cell* **2015**, *14*, 1017–1042. [CrossRef]
42. González-Hourcade, M.; Braga, M.R.; del Campo, E.M.; Ascaso, C.; Patinõ, C.; Casano, L.M. Ultrastructural and biochemical analyses reveal cell wall remodelling in lichen-forming microalgae submitted to cyclic desiccation-rehydration. *Ann. Bot.* **2020**, *125*, 459–469. [CrossRef]
43. Bischoff, H.W.; Bold, H.C. Phycological studies. IV. In *Some Soil Algae from Enchanted Rock and Related Algal Species*; University of Texas Publications 6318: Austin, TX, USA, 1963.
44. Bold, H.C.; Parker, B.C. Some supplementary attributes in the classification of *Chlorococcum* species. *Arch. Mikrobiol.* **1962**, *42*, 267–288. [CrossRef]
45. Schindelin, J.; Arganda-Carreras, I.; Frise, E.; Kaynig, V.; Longair, M.; Pietzsch, T.; Preibisch, S.; Rueden, C.; Saalfeld, S.; Schmid, B.; et al. Fiji: An open-source platform for biological-image analysis. *Nat. Methods* **2012**, *9*, 676–682. [CrossRef] [PubMed]
46. Muggia, L.; Pérez-Ortega, S.; Kopun, T.; Zellnig, G.; Grube, M. Photobiont selectivity leads to ecological tolerance and evolutionary divergence in a polymorphic complex of lichenized fungi. *Ann. Bot.* **2014**, *114*, 463–475. [CrossRef] [PubMed]
47. Hayles, M.F.; de Winter, D.A.M. An introduction to cryo-FIB-SEM cross-sectioning of frozen, hydrated Life Science samples. *J. Microsc.* **2021**, *281*, 138–156. [CrossRef] [PubMed]
48. Gasulla, F.; de Nova, P.G.; Esteban-Carrasco, A.; Zapata, J.M.; Barreno, E.; Guéra, A. Dehydration rate and time of desiccation affect recovery of the lichenic algae *Trebouxia erici*: Alternative and classical protective mechanisms. *Planta* **2009**, *231*, 195–208. [CrossRef] [PubMed]
49. Candotto Carniel, F.; Zanelli, D.; Bertuzzi, S.; Tretiach, M. Desiccation tolerance and lichenization: A case study with the aeroterrestrial microalga *Trebouxia* sp. (Chlorophyta). *Planta* **2015**, *242*, 493–505. [CrossRef]
50. Banchi, E.; Candotto Carniel, F.; Montagner, A.; Petruzzellis, F.; Pichler, G.; Giarola, V.; Bartels, D.; Pallavicini, A.; Tretiach, M. Relation between water status and desiccation-affected genes in the lichen photobiont *Trebouxia gelatinosa*. *Plant Physiol. Biochem.* **2018**, *129*, 189–197. [CrossRef]
51. Gasulla, F.; Jain, R.; Barreno, E.; Guéra, A.; Balbuena, T.S.; Thelen, J.J.; Oliver, M.J. The response of *Asterochloris erici* (Ahmadjian) Skaloud et Peksa to desiccation: A proteomic approach. *Plant Cell Environ.* **2013**, *36*, 1363–1378. [CrossRef]
52. Scheidegger, C.; Schroeter, B. Structural and Functional Processes during Water Vapour Uptake and Desiccation in Selected Lichens with Green Algal Photobionts. *Planta* **1995**, *197*, 399–409. [CrossRef]
53. González-Hourcade, M.; del Campo, E.M.; Casano, L.M. The under-explored extracellular proteome of aero-terrestrial microalgae provides clues on different mechanisms of desiccation tolerance in non-model organisms. *Microb. Ecol.* **2021**, *81*, 437–453. [CrossRef]
54. Bruñas Gómez, I.; Casale, M.; Barreno, E.; Catalá, M. Near-infrared metabolomic fingerprinting study of lichen thalli and phycobionts in culture: Aquaphotomics of *Trebouxia lynnae* dehydration. *Microorganisms* **2022**, *10*, 2444. [CrossRef]
55. Kalinina, N.O.; Makarova, S.; Makhotenko, A.; Love, A.J.; Taliansky, M. The multiple functions of the nucleolus in plant development, disease and stress responses. *Front. Plant Sci.* **2018**, *9*, 132. [CrossRef]
56. Stępiński, D. Functional ultrastructure of the plant nucleolus. *Protoplasma* **2014**, *251*, 1285–1306. [CrossRef]
57. Tukaj, Z.; Baścik-Remisiewicz, A.; Skowroński, T.; Tukaj, C. Cadmium effect on the growth, photosynthesis, ultrastructure and phytochelatin content of green microalga *Scenedesmus armatus*: A study at low and elevated CO_2 concentration. *Environ. Exp. Bot.* **2007**, *60*, 291–299. [CrossRef]

58. Leonardo, T.; Farhi, E.; Pouget, S.; Motellier, S.; Boisson, A.-M.; Banerjee, D.; Rébeillé, F.; den Auwer, C.; Rivasseau, C. Silver accumulation in the green microalga *Coccomyxa actinabiotis*: Toxicity, in situ speciation, and localization investigated using synchrotron XAS, XRD, and TEM. *Environ. Sci. Technol.* **2016**, *50*, 359–367. [CrossRef]
59. Pulich, W.M.; Ward, C.H. Physiology and ultrastructure of an oxygen-resistant *Chlorella* mutant under heterotrophic conditions. *Plant Physiol.* **1973**, *51*, 337–344. [CrossRef]
60. Atkinson, A.W.; John, P.C.L.; Gunning, B.E.S. The growth and division of the single mitochondrion and other organelles during the cell cycle of *Chlorella*, studied by quantitative stereology and three dimensional reconstruction. *Protoplasma* **1974**, *81*, 77–109. [CrossRef]
61. Dempsey, G.P.; Lawrence, D.; Cassie, V. The ultrastructure of *Chlorella minutissima* Fott et Nováková (*Chlorophyceae*, Chlorococcales). *Phycologia* **1980**, *19*, 13–19. [CrossRef]
62. Guo, W.; Feng, L.; Wang, Z.; Guo, J.; Park, D.; Carroll, B.L.; Zhang, X.; Liu, J.; Cheng, J. In-situ high-resolution 3D imaging combined with proteomics and metabolomics reveals enlargement of subcellular architecture and enhancement of photosynthesis pathways in nuclear-irradiated *Chlorella pyrenoidosa*. *Chem. Eng. J.* **2022**, *430*, 133037. [CrossRef]
63. Wolf, J.M.; Espadas-Moreno, J.; Luque-Garcia, J.L.; Casadevall, A. Interaction of *Cryptococcus neoformans* extracellular vesicles with the cell wall. *Eukaryot. Cell* **2014**, *13*, 1484–1493. [CrossRef]
64. Honegger, R. Cytological aspects of the mycobiont–phycobiont relationship in lichens. *Lichenologist* **1984**, *16*, 111–127. [CrossRef]
65. Arakawa, S.; Kanaseki, T.; Wagner, R.; Goodenough, U. Ultrastructure of the foliose lichen *Myelochroa leucotyliza* and its solo fungal and algal (*Trebouxia* sp.) partners. *Algal. Res.* **2022**, *62*, 102571. [CrossRef]